

THIS IS AN AUTHOR-CREATED POSTPRINT VERSION.

Disclaimer: This work has been accepted for publication in *21st IEEE International Conference on Factory Communication Systems (WFCS 2025)*.

Copyright: © 2025 IEEE. Personal use of this material is permitted. Permission from IEEE must be obtained for all other uses, in any current or future media, including reprinting/republishing this material for advertising or promotional purposes, creating new collective works, for resale or redistribution to servers or lists, or reuse of any copyrighted component of this work in other works.

Empirical Analysis of the Impact of 5G Jitter on Time-Aware Shaper Scheduling in a 5G-TSN Network

Pablo Rodriguez-Martin^{*†}, Oscar Adamuz-Hinojosa^{*†}, Pablo Muñoz^{*†},
Julia Caleya-Sanchez^{*†}, Jorge Navarro-Ortiz^{*†}, Pablo Ameigeiras^{*†}

^{*}Department of Signal Theory, Telematics and Communications, University of Granada.

[†]Research Center on Information and Communication Technologies, University of Granada.

Email: {pablorodrigar, oadamuz, pabloml, jcaleyas, jorgenavarr, pameigeiras}@ugr.es^{*†}

Abstract—Deterministic communications are essential for industrial automation, ensuring strict latency requirements and minimal jitter in packet transmission. Modern production lines, specializing in robotics, require higher flexibility and mobility, which drives the integration of Time-Sensitive Networking (TSN) and 5G networks in Industry 4.0. TSN achieves deterministic communications by using mechanisms such as the IEEE 802.1Qbv Time-Aware Shaper (TAS), which schedules packet transmissions within precise cycles, thereby reducing latency, jitter, and congestion. 5G networks complement TSN by providing wireless mobility and supporting ultra-Reliable Low-Latency Communications. However, 5G channel effects such as fast fading, interference, and network-induced latency and jitter can disrupt TSN traffic, potentially compromising deterministic scheduling and performance. This paper presents an empirical analysis of 5G network latency and jitter on IEEE 802.1Qbv performance in a 5G-TSN network. We evaluate the impact of 5G integration on TSN's deterministic scheduling through a testbed combining IEEE 802.1Qbv-enabled switches, TSN translators, and a commercial 5G system. Our results show that, with proper TAS configuration in the TSN switch aligned with the 5G system, jitter can be mitigated, maintaining deterministic performance.

Index Terms—TSN, IEEE 802.1Qbv, 5G, jitter, Industry 4.0, testbed.

I. INTRODUCTION

The advent of 5th Generation (5G) networks and the emerging vision for 6th Generation (6G) networks are driven by the need to support a broad range of applications, including Connected Robotics and Autonomous Systems (CRAS) [1]. These systems—encompassing autonomous and collaborative robots, drones, and other intelligent agents—have the potential to revolutionize multiple industry verticals, with industrial automation standing out as a key beneficiary. The integration of cutting-edge technologies such as the Internet of Things (IoT), Cyber-Physical System (CPS), cloud computing, and Artificial Intelligence (AI) is expected to elevate industrial automation to unprecedented levels of efficiency and intelligence.

This work has been financially supported by the Ministry for Digital Transformation and of Civil Service of the Spanish Government through TSI-063000-2021-28 (6G-CHRONOS) project, and by the European Union through the Recovery, Transformation and Resilience Plan - NextGenerationEU. Additionally, this publication is part of grant PID2022-137329OB-C43 funded by MICIU/AEI/ 10.13039/501100011033 and part of FPU Grant 21/04225 funded by the Spanish Ministry of Universities.

A fundamental requirement for industrial automation applications is the ability to provide communication services that meet stringent constraints in terms of data rate, reliability, and latency [2]. This necessitates network architectures capable of providing efficient, low-latency, highly reliable, and deterministic communications. To address these needs, the IEEE has developed the Time-Sensitive Networking (TSN) standards, which introduce key capabilities such as time synchronization, stream reservation, traffic shaping, scheduling, preemption, traffic classification, and seamless redundancy. These features are essential for ensuring the deterministic performance required in industrial automation environments.

While TSN standards ensure determinism and reliability in wired networks, 5G/6G systems extend these capabilities by enabling mobility, wide-area coverage, and scalability. Integrating 5G/6G systems with TSN [3] has emerged as a promising solution to meet the stringent communication demands of CRAS and industrial automation. In this setup, production lines in a factory connect wirelessly to the 5G/6G system, which then interfaces with the enterprise edge-cloud through TSN switches. However, this integration presents significant challenges due to fundamental differences between wired TSN networks and wireless 5G/6G systems. A key challenge lies in *incorporating TSN's IEEE 802.1Qbv standard, which defines a Time-Aware Shaping (TAS) for deterministic packet scheduling*. The introduction of 5G/6G systems into a TSN-based industrial network introduces additional latency and jitter compared to traditional TSN switches and wired links. These impairments stem from the dynamic and uncertain nature of wireless transmission and the time-varying processing delays within 5G/6G network nodes. The jitter introduced by 5G/6G may cause packets to not be transmitted according to the TAS schedules, resulting in potential failures in industrial processes. Thus, a dejittering mechanism based on TAS is needed to maintain the deterministic behavior in the network.

A. Related work

Currently, the research on integration between 5G and TSN networks is in its early stages. The works in [4] [5] provide a comprehensive analysis of the current and future research

directions on 5G-TSN integration. From an architectural perspective, it is well established that the 5G system behaves as a TSN logical switch, as discussed in [6] [7]. Several works address time synchronization [8] and 5G-TSN QoS mapping [9] as key functions for this logical switch model. However, there are still some open issues to be addressed. A crucial issue is related to the non-deterministic behavior of the 5G system and its impact on the TSN scheduled traffic. This challenge has been addressed in [10] [11], where evaluations are carried out by simulation tools. In relation to this, there is also a lack of functional testbeds to conduct tests under realistic conditions. Some preliminary results on this are presented in [12], revealing a significant dependence on the native capabilities of the 5G system and a need for a global schedule in the integrated network. Thus, further research is required to analyze the impact of the 5G capabilities and constraints.

B. Contributions

In this work, we present an empirical analysis of the impact of 5G network latency and jitter on the performance of IEEE 802.1Qbv in an integrated 5G-TSN network. Our key contributions are as follows:

- C1 We analyze the Downlink (DL) transmission in a 5G-TSN network and evaluate how the integration of the 5G system affects the deterministic scheduling of IEEE 802.1Qbv.
- C2 We develop an experimental testbed integrating TSN and 5G technologies, including IEEE 802.1Qbv-enabled switches, TSN translators, and a commercial 5G system.
- C3 We identify the key configuration parameters required to optimize IEEE 802.1Qbv integration in a 5G-TSN environment and analyze the associated constraints.

Our results demonstrate that, with an appropriate configuration of the TAS schedule in the TSN switches, it is possible to mitigate the 5G jitter and maintain deterministic performance.

The paper is structured as follows. Section II provides background on industrial 5G-TSN networks. Section III introduces the system model, while Section IV analyzes the impact of 5G jitter on TAS scheduling. Section V describes the testbed and experimental setup. In Section VI, we present the performance results. Finally, Section VII summarizes the key conclusions and outlines directions for future work.

II. BACKGROUND ON 5G-TSN INDUSTRIAL NETWORKS

In this section, we provide background on the network architecture, device synchronization, deterministic traffic shaping, and the considered industrial applications.

A. Network Segments for Industry Automation

As depicted in Fig. 1, three connectivity segments may be identified in a 5G-TSN-based industrial network [3]:

- **Edge/Cloud Room:** serves as a centralized management layer, hosting control functions such as those traditionally executed by Programmable Logic Controllers (PLCs). These can be deployed on dedicated hardware or general-purpose servers. Additionally, management tasks—including monitoring, data collection, and analytics—are handled by

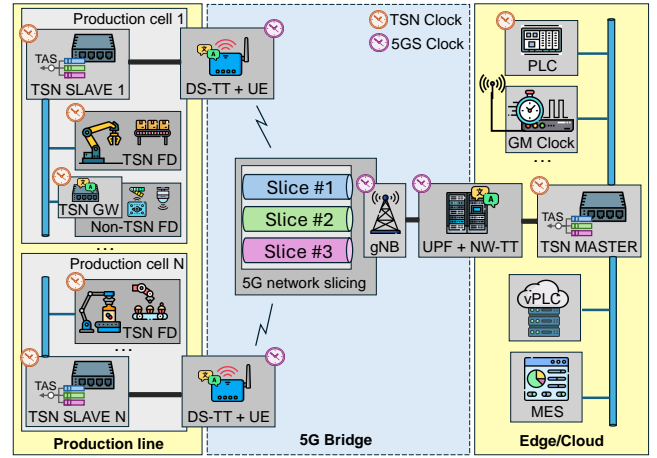


Fig. 1. 5G-TSN network architecture in an Industry 4.0 factory.

systems like Manufacturing Execution System (MES). This segment also incorporates a server providing the TSN Grandmaster (GM) clock reference to be distributed, typically derived from Global Navigation Satellite System (GNSS).

- **5G System:** following 3rd Generation Partnership Project (3GPP) TS 23.501 (v19.0.0) [13], the 5G system integrates into the TSN network as one or more virtual TSN switches, with User Plane Functions (UPFs) and User Equipments (UEs) as endpoints. The UE connects to the UPF via the next generation Node B (gNB), which provides wireless connectivity. The TSN translators, i.e., Network-side Translator (NW-TT) and Device-side Translator (DS-TT), integrated within the UPF and UE, respectively; handle wireless 5G network timing correction functionalities. This work focuses solely on the data plane, excluding control functions, and considers a single UE per production line, which provides wireless 5G connectivity between production lines and enables access to the edge/cloud room.
- **Production Line:** it includes multiple Field Devices (FDs) and local PLCs for distributed control. FDs report status and measurements to centralized PLCs, enabling hierarchical decision-making. The production line is divided into cells, each connected to a TSN slave switch that receives the clock signal from the TSN master via the 5G system and redistributes it to the FDs in its production line.

Focusing on traffic management, traffic from various industrial applications may be isolated in the 5G system into distinct Quality of Service (QoS) flows. Each flow is treated differently in terms of resource allocation, based on its specific requirements for latency, reliability, bandwidth, and priority, as defined in 3GPP TS 23.501 (v19.0.0). To harmonize QoS management between TSN and 5G system, packet filters at the UE and UPF map Ethernet packets to specific 5G QoS flows based on their Priority Code Point (PCP) values. In Uplink (UL), the UE applies packet filtering to classify outgoing packets before they enter the 5G network. In DL, the UPF performs this filtering to ensure packets are assigned to the appropriate 5G QoS flow before reaching the UE. The PCP

is a field within the Virtual Local Area Network (VLAN) tag used to classify Ethernet frames into different priority levels. Additionally, one or more 5G QoS flows can be mapped to a specific network slice, enabling the reservation of a dedicated amount of radio resources for that slice, and thus for those 5G QoS flows.

B. Synchronization in 5G-TSN Network

Time synchronization is essential in a 5G-TSN network to ensure the deterministic execution of industrial automation processes. In this context, a TSN network typically includes a TSN master switch that distributes the GM clock reference via Precision Time Protocol (PTP) messages to one or more TSN slave switches in the production lines. These TSN slaves compute the clock offset from the TSN master switch to adjust their clocks accordingly. We assume the 5G system operates as a PTP Transparent Clock (TC) [14], meaning that the 5G bridge forwards synchronization messages without modifying the timestamps but correcting delay between TSN translators.

Discrepancies in the clocks of different devices within the 5G-TSN network can occur, preventing the devices from updating their clocks accurately. This leads to clock drifts, typically in the order of hundreds of nanoseconds. 3GPP TS 22.104 [15] specifies a maximum delay of 900 ns must be guaranteed in the industrial network for 5G systems. However, the synchronization error is several orders of magnitude smaller than the 5G jitter, which is in the order of milliseconds. Therefore, we assume the synchronization error is negligible.

C. IEEE 802.1Qbv Time-Aware Shaper

IEEE 802.1Qbv is a TSN standard that defines the TAS mechanism, enabling time-aware scheduling of Layer 2 frames at each TSN switch's egress port while accounting for different QoS levels [16]–[18]. TAS operates based on the PCP field in the IEEE 802.1Q header, where frames are assigned a 3-bit priority value, i.e. from 0 to 7, and mapped to one of eight First-Input First-Output (FIFO) queues. These queues, located at each switch's egress port, correspond to distinct traffic classes, ensuring differentiated QoS enforcement.

To regulate frame transmission from these queues, each egress port is associated with a Gate Control List (GCL), which determines the eligibility of each queue for transmission. Each queue has its own gate, and traffic scheduling is organized into cyclical *transmission windows*, during which one or more gates open to allow transmission from the respective queues. Within each transmission window, if multiple gates are open simultaneously, frames from the highest-priority queue are transmitted first, followed by frames from the next highest-priority queue, and so on, until all eligible queues have been served. For TAS, we assume one gate at a time.

D. Industrial applications

In industrial networks, most of the traffic is delay-critical, as defined in [3]. It can be classified as *isochronous* or *cyclic*.

Isochronous applications require strictly periodic and coordinated packet transmissions, with delays shorter than their

execution period, a.k.a. *application cycle*. These high-priority applications, common in motion control, automotive systems, AI vision, and Audio Video Bridging (AVB); rely on synchronized clocks across all TSN switches. Each switch and its TAS scheduling must be time-aligned to prevent delays, ensuring packets reach the processing unit (e.g., PLC at the edge) on time. In contrast, cyclic applications also follow a periodic transmission pattern but are less stringent about synchronization among TSN switches. These applications can tolerate bounded jitter, and times may vary depending on when the industrial process is initiated. Examples include industrial sensor polling, where data is periodically collected and processed. This work focuses on general cyclic applications.

III. SYSTEM MODEL

In this section, we first present the network model, which defines the fundamental structure of the industrial network under consideration. Next, we introduce the traffic model, describing the characteristics of the considered industrial data flows. Finally, we outline the TAS model, detailing its role within the industrial network.

A. Network Model

We consider an industrial network \mathcal{V} comprising two TSN switches: a TSN master MS and a TSN slave SL, where $MS, SL \in \mathcal{V}$, as depicted in Fig. 2. The processing delay of these TSN switches, i.e., d_{MS}^{proc} and d_{SL}^{proc} , represent the time required to internally transfer a packet to an output port's queue. Additionally, the output ports of TSN switches MS and SL operate with a macrotick of m seconds.

The transmission between TSN switches MS and SL is carried out by several links and devices. The equipment supporting this packet transmission consists of two TSN translators, i.e., NW-TT and DS-TT, as well as the UE, the gNB and the 5G core, thus shaping our 5G bridge. Both NW-TT and DS-TT are denoted as NW and DS, respectively, with $NW, DS \in \mathcal{V}$. Both TSN translators have processing delays denoted as d_{NW}^{proc} and d_{DS}^{proc} . Every link is denoted with ε , i.e. $\varepsilon_{MS,NW}, \varepsilon_{DS,SL} \in \mathcal{E}$.

Since links are bidirectional, we distinguish between the UL and DL by swapping the subscript order, i.e., $\varepsilon_{NW,MS}, \varepsilon_{SL,DS} \in \mathcal{E}$. The bandwidth of each link is given by b , i.e., $b_{MS,NW}$ and $b_{DS,SL}$, respectively. The bandwidth is established by the

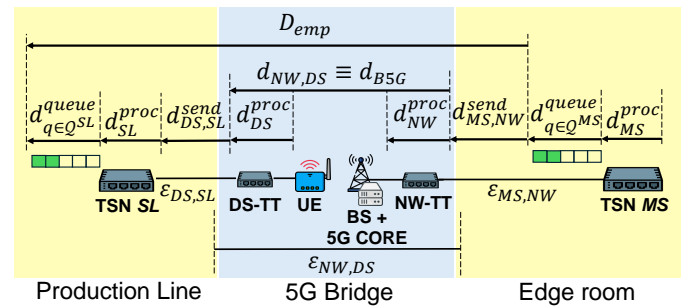


Fig. 2. 5G-TSN network elements and associated delays in a DL transmission.

ports' capacities. In terms of delay, the *propagation delays* are determined by $d_{MS,NW}^{prop}$ and $d_{DS,SL}^{prop}$. The total *sending delay* is equivalent to adding the *transmission delay* to the propagation delay, i.e., $d_{MS,NW}^{send} = d_{MS,NW}^{prop} + l_x/b_{MS,NW}$, where l_x is the length of the bit string to be transmitted. Similarly, $d_{DS,SL}^{send} = d_{DS,SL}^{prop} + l_x/b_{DS,SL}$.

The 5G bridge, functioning as a TSN non-time-aware device, forwards packets between virtual ports, i.e., NW-TT and DS-TT; without implementing any TAS configuration. It comprises both TSN translators and the 5G system wireless link $\varepsilon_{NW,DS} \in \mathcal{E}$, which defines the inner connection between 5G system elements.

For wired connections, the behavior is typically symmetric between UL and DL in terms of data rate and latency, e.g., $b_{DS,SL} = b_{SL,DS}$ and $d_{DS,SL}^{send} = d_{SL,DS}^{send}$. In contrast, for wireless connections in the 5G bridge, both data rate and latency must be measured separately for UL and DL due to inherent capacity asymmetry, i.e., $b_{NW,DS} \neq b_{DS,NW}$ and $d_{NW,DS} \neq d_{DS,NW}$. For simplicity, we denote this 5G bridge delay as d_{BSG} . We also denote $b_{MS,SL}$ as the composed capacity of all wired and wireless links in series from MS to SL, likely equal to the bottleneck capacity of 5G bridge in DL, $b_{NW,DS}$.

Furthermore, we define the queuing delay for the queue $q \in \mathcal{Q}^x$ at the output port of the TSN switches, where $x = \{MS, SL\}$ denotes a specific TSN switch. The queuing delay at the TSN switch MS for queue q is denoted as $d_{q \in \mathcal{Q}^{MS}}^{queue}$, and at the TSN switch SL for queue q as $d_{q \in \mathcal{Q}^{SL}}^{queue}$.

B. Traffic Model

In this work, we focus on the DL traffic, although the formulation presented hereafter can also be extrapolated to the UL direction. We consider two types of traffic streams: a *delay-critical* stream, denoted as $DC \in \mathcal{S}$, and a *best-effort* stream, denoted as $BE \in \mathcal{S}$, where \mathcal{S} is the set of streams.

For the delay-critical stream DC, we assume a set of N_{DC} packets that are transmitted in a burst, with a fixed *application cycle* T_{DC}^{app} between transmissions. The packet size l_{DC} for traffic stream DC is considered constant. Additionally, we define the packet delay budget D_{DC} for the delay-critical stream DC within the industrial network requirements. For the best-effort stream BE, we assume that packets are transmitted at a constant data rate R_{BE} . The packet size l_{BE} for BE stream is also constant. Additionally, no packet delay budget is defined for the best-effort stream BE.

We consider a 5G network slice associated to a PCP for each kind of traffic. Thus, ultra-Reliable and Low-Latency Communications (uRLLC) slice is reserved for DC traffic while enhanced Mobile BroadBand (eMBB) is for BE traffic.

C. TAS model

The *network cycle* [19] is a fixed and recurring time interval during which the scheduled transmissions from the considered output port queues are organized and executed according to a predefined GCL schedule. Each network cycle consists of multiple *transmission windows*, ensuring deterministic communication by assigning exclusive transmission opportunities

to different traffic classes. The duration of the network cycle corresponds to the Greatest Common Divisor (GCD) of all *application cycles* involved, given by $T_C = \text{GCD}(T_s^{app}) \forall s \in \mathcal{S}$. In our study, since only one *delay-critical* stream DC is constrained by an application cycle of T_{DC}^{app} , it results in $T_C = T_{DC}^{app}$.

We assume the GCL enforces exclusive stream transmission, allowing only one queue to transmit at a *transmission window*. Focusing on the *delay-critical* stream DC, we examine its transmission from TSN switch MS to TSN switch SL. Specifically, we consider the corresponding queue $q \in \mathcal{Q}^{MS}$ at the output port of TSN switch MS. The GCL for this port must be configured based on the *network cycle* T_C , as outlined in Eq. (1). The binary variable $G_{MS,SL,q \rightarrow DC}(t)$ takes the value 1 when the gate is open and 0 otherwise. The gate opens periodically during each *network cycle* of duration T_C . Focusing on the first network cycle, i.e., $n = 0$, the variables $t_{1,DC}^{MS,SL}$ and $t_{2,DC}^{MS,SL}$ define the time instants at the *transmission window* for the traffic stream DC, thereby establishing when the gate is open or closed, respectively.

$$G_{MS,SL,q \rightarrow DC}(t) = \begin{cases} 1, & nT_C + t_{1,DC}^{MS,SL} < t \leq nT_C + t_{2,DC}^{MS,SL}, \\ & \forall n \in \mathbb{N} \cup \{0\} \\ 0, & \text{otherwise} \end{cases} \quad (1)$$

Based on that, we can define the duration of the *transmission window* as $w_{DC}^{MS,SL} = t_{2,DC}^{MS,SL} - t_{1,DC}^{MS,SL}$. The duration $w_{DC}^{MS,SL}$ of the *transmission window* for the traffic stream DC must be at least as large as the transmission time required for the burst of N_{DC} packets and lower than the *network cycle* T_C as defined in Eq. (2). The lower size bound is determined by multiplying the number of packets N_{DC} by their size l_{DC} , and then dividing by the link's bandwidth $b_{MS,SL}$.

$$N_{DC} \frac{l_{DC}}{b_{MS,SL}} \leq w_{DC}^{MS,SL} < T_C \quad (2)$$

Note that, if the previous condition is not met, the following consequences may arise. If the *transmission window* is shorter than its lower bound, i.e., $w_{DC}^{MS,SL} < N_{DC}l_{DC}/b_{MS,SL}$, it means insufficient time to transmit the N_{DC} packets of the traffic flow DC. As a result, the packets that remain queued are transmitted with an extra delay that is a multiple of the *network cycle* duration T_C , since they would accumulate and be transmitted in the subsequent network cycles, leading to a packet queueing effect. On the other hand, if the *transmission window* exceeds the upper bound, i.e., $w_{DC}^{MS,SL} > T_C$, the scheduling would not be approachable as it takes place during the whole network cycle and no other streams can be transmitted. Moreover, if $w_{DC}^{MS,SL}$ is not well fitted, the elapsed time between the end of the transmission of the last packet and the end of the network cycle would be wasted.

In our study, the remaining time until the completion of the *network cycle* T_C is used to transmit data from the *best-effort* stream $BE \in \mathcal{S}$, followed by a guard band to avoid frame collisions. This means $T_C = w_{DC}^{MS,SL} + w_{BE}^{MS,SL} + t_{GB}$, where $w_{BE}^{MS,SL}$ is the *transmission window* for the *best-effort* stream BE and t_{GB} the guard band time.

After establishing the TAS model, a mathematical analysis of its behavior in a 5G-TSN network is presented below.

IV. ANALYSIS OF 5G JITTER ON TAS SCHEDULING

The traffic streams $DC, BE \in \mathcal{S}$ will follow a path of network nodes until reaching its destination as illustrated in Fig. 2. This path is defined as $\mathcal{P}_{nodes} \equiv \{MS, NW, DS, SL\}$, where $MS, NW, DS, SL \in \mathcal{V}$. Additionally, the list of links that connect these nodes is defined as $\mathcal{P}_{links} \equiv \{\varepsilon_{MS,NW}, \varepsilon_{NW,DS}, \varepsilon_{DS,SL}\}$, where $\varepsilon_{MS,NW}, \varepsilon_{NW,DS}, \varepsilon_{DS,SL} \in \mathcal{E}$. The total packet transmission delay D_{tot} for a stream $s \in \mathcal{S}$ following this path is described by Eq. 3.

$$D_{tot} = \sum_{v \in \{MS, SL\}} (d_{q \in Q^v}^{queue} + d_v^{proc}) + d_{MS,NW}^{send} + d_{B5G} + d_{DS,SL}^{send} \quad (3)$$

In our work, we focus on an analysis of the 5G jitter on TAS scheduling. The jitter is defined as the variation of the packet transmission delay in the 5G network due to channel effects as fast-fading. To properly capture the impact of the 5G jitter on TAS scheduling, we empirically measure the packet transmission delay D_{emp} since the TSN MS sends the packet until this packet is departed from the TSN SL. Based on that, the packet transmission delay D_{emp} can be defined as Eq. (4) shows. Note that $K = d_{MS,NW}^{send} + d_{DS,SL}^{send} + d_{SL}^{proc}$ represents the sum of those delay terms that are constant, being the remaining terms variable for each packet. The term d_{B5G} includes the 5G jitter. Concerning $d_{q \in Q^{SL}}^{queue}$, its variability depends on factors such as: (a) the time the packet enters the corresponding queue, (b) the current queue occupation, and (c) if the *transmission window*—and thus, the gate—is open or not for such queue.

$$\begin{aligned} D_{emp} &= d_{MS,NW}^{send} + d_{B5G} + d_{DS,SL}^{send} + d_{SL}^{proc} + d_{q \in Q^{SL}}^{queue} = \\ &= K + d_{B5G} + d_{q \in Q^{SL}}^{queue} \end{aligned} \quad (4)$$

To reduce the variability of the delay term $d_{q \in Q^{SL}}^{queue}$, the sequence of GCL events needs to be coordinated among the TSN switches $MS, SL \in \mathcal{V}$. Specifically, the receiving TSN switch SL must apply an offset δ to the beginning of the *network cycle* concerning the transmitter TSN switch MS. The use of this offset aims to ensure the received packets from the TSN switch MS arrive at the TSN SL before a *transmission window* starts. To achieve this, the offset δ must have the lower bound defined in Eq. (5). Specifically, this lower bound is the sum of all the packet propagation delays from this packet leaves the TSN MS until it reaches the TSN SL, including the processing delay d_{SL}^{proc} required by the TSN SL to put this packet into the corresponding queue. Note that the delays $d_{MS,NW}^{send}$, $d_{DS,SL}^{send}$ and d_{SL}^{proc} are constant whereas d_{B5G} is variable due to the fluctuating packet transmission time in the 5G network, caused by wireless channel effects such as fast fading. For such reason, Eq. (5) considers the maximum value of the delay d_{B5G} .

$$\delta \geq d_{MS,NW}^{send} + \max\{d_{B5G}\} + d_{DS,SL}^{send} + d_{SL}^{proc} \quad (5)$$

The offset δ must be set considering the lower bound defined in Eq. (5). In this lower bound, the only term that

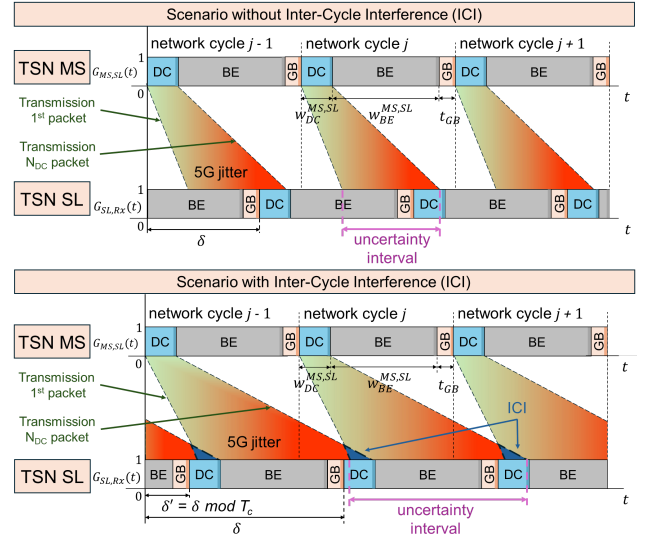


Fig. 3. 5G jitter effect over TAS cycles according to its uncertainty interval. Note that we assume a node Rx $\in \mathcal{V}$ attached to TSN switch SL.

is variable is the propagation delay through the 5G bridge, i.e., d_{B5G} . In this work, we define the *uncertainty interval* as the range of values which the variable d_{B5G} can take. As shown in Fig. 3, the impact of 5G jitter on TAS depends on the configured *transmission windows* $w_{DC}^{MS,SL}$, $w_{BE}^{MS,SL}$ for the TSN switches MS and SL; and the *network cycle* T_C . When the *network cycle* exceeds the uncertainty interval, i.e., $T_C > d_{B5G}$, the TSN slave can schedule their enqueued packets by simply considering the offset δ with respect to the TSN master's scheduling. However, shorter *network cycles*, i.e., $T_C < d_{B5G}$, and offset δ misalignments may cause packets to arrive before or after their reserved *transmission windows*, leading to an increase in the packet latency D_{tot} . We define this phenomenon as Inter-Cycle Interference (ICI), which can prevent packets from reaching their destinations on time.

Since the packet transmission delay in a 5G system, i.e., d_{B5G} , is not strictly bounded, it is essential to consider its statistical distribution. In our work, we define the *uncertainty interval* by establishing a statistical upper bound based on a specific percentile p of the Cumulative Distribution Function (CDF) $F_{B5G}(\cdot)$ of this delay. Specifically, we define the upper bound $\hat{d}_{B5G} = F_{B5G}^{-1}(p)$. For example, we may set the upper bound \hat{d}_{B5G} such that 99.9% of the packets (i.e., $p = 0.999$) are transmitted below this threshold. Based on that and considering Eq. (5), we define the offset δ as Eq. (6) shows. The network cycle offset δ' is calculated as $\delta' = \delta \bmod T_C$.

$$\delta = d_{MS,NW}^{send} + \hat{d}_{B5G} + d_{DS,SL}^{send} + d_{SL}^{proc} = K + \hat{d}_{B5G} \quad (6)$$

V. TESTBED AND EXPERIMENTAL SETUP

In this section, we describe the implemented 5G-TSN testbed and the considered experimental setup.

A. Testbed Description

To validate our solution, we implemented the testbed depicted in Fig. 4. It consists of: (i) a 5G system, (ii) five TSN

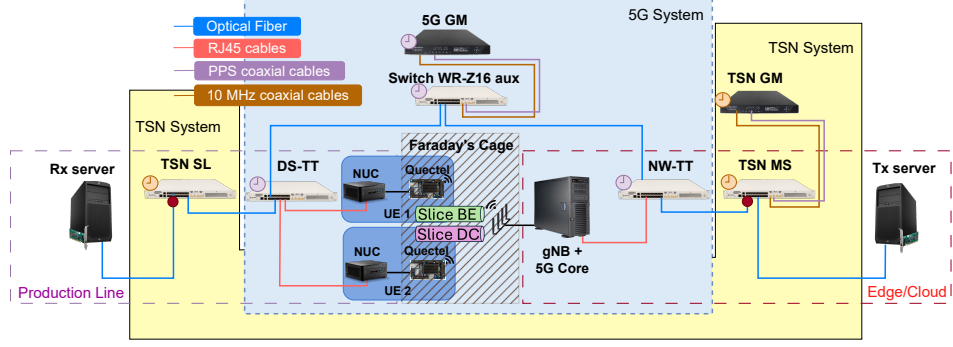


Fig. 4. Proof of concept equipment and evaluated network scenario.

switches, (iii) two GNSS time synchronization servers, and (iv) two servers acting as end devices.

5G System. The 5G network consists of a single Base Station (BS) and a 5G core, both built on a PC with two 50 MHz PCIe Software Defined Radio (SDR) Amarisoft cards and an AMARI NW 600 license. BS operates in the $n78$ frequency band, using a 30 kHz Sub-Carrier Spacing (SCS) and Time Division Duplex (TDD) mode. Hence, data transmission is organized into time slots. In this work, we use the 4D-2S-4U TDD pattern, which follows a repeating pattern of four consecutive slots for DL and four consecutive slots for UL, with two flexible slots in between. The UE consists of a Quectel RM500Q-GL modem connected to an Intel NUC 10 NUC10i7FNKN. The Intel NUC has a i7-10710U processor, 16 GB of RAM, and a 512 GB SSD, running Ubuntu 22.04. Two UEs are deployed in this setup.

Experiments are conducted inside a LABIFIX Faraday cage, where the BS antennas are connected to one of the SDR via SMA connectors, and the Quectel modems connect via USB to the NUC thus forming the UEs.

The UE does not support Ethernet-based Packet Data Unit (PDU) sessions. Therefore, the 5G network is based on IP transport. Thus, to enable the transmission of industrial automation Layer 2 traffic, a Virtual Extensible LAN (VxLAN)-based tunneling mechanism is implemented. There are two different VxLANs, one for each PCP-slice tuple. Furthermore, two distinct Data Network Names (DNNs) have been configured: one for DC communications and PTP messages, and another for BE traffic. The traffic from one DNN is mapped to a uRLLC slice, while the traffic from the other DNN is mapped to an eMBB slice. The uRLLC and eMBB slices are defined based on the Slice/Service Type (SST) parameter of the Single Network Slice Selection Assistance Information (S-NSSAI), as specified by 3GPP, where $SST=1$ corresponds to eMBB and $SST=2$ corresponds to uRLLC. Despite previous works consider one TSN translator per UE and slice, we opt for a single pair of TSN translators to simplify this setup.

TSN Network. The TSN switches are based on Safran's WR-Z16 switches, with one acting as a TSN MS, another as the TSN SL, and two switches functioning as TSN translators,

i.e., NW-TT and DS-TT. The TSN MS is directly connected to Safran's SecureSync 2400 server to distribute a precise time reference, i.e., GM clock, to TSN SL. An auxiliary TSN switch, supported by another SecureSync 2400, enables the 5G GM clock distribution between TSN translators.

TSN Switch Capabilities. WR-Z16 is based on Xilinx Zynq 7000 series Field-Programmable Gate Array (FPGA) and a 1 GHz dual ARM Cortex A9 core. This allows high switching rates and very low processing delays, with configurations running on top of a Linux-based OS. Each WR-Z16 TSN switch supports IEEE 802.1Qbv TAS and VLANs. It counts with 16 1 GbE Small Form-factor Pluggable (SFP) configurable timing ports that can assume the role of master or slave for PTP transmission. Each port counts with 4 queues. Their sizes are limited to 6.8 kB, so shorter bitrates for DC communications can be tested. Additionally, ports count on timestamping probes for measuring high-accuracy latencies between TSN switches. The TAS macrotick is 16 nanoseconds.

Testbed Clock Synchronization. Time synchronization between the TSN GM clock server and the TSN MS switch is achieved through coaxial cables carrying the Pulse Per Second (PPS) and 10 MHz signals. Similarly, the auxiliary WR-Z16 switch synchronizes with the 5G GM clock server via coaxial cables to distribute the time reference between NW-TT and DS-TT. Thus, we assume very high accuracy synchronization in the 5G segment. Synchronization error between these devices is left for future research work. In our testbed, the TSN MS and the TSN SL use User Datagram Protocol (UDP) over IPv4 in unicast mode with the End-to-end (E2E) delay measurement mechanism to encapsulate PTP frames. The PTP transmission rate is set to 1 packet per second.

End devices. Two servers running Ubuntu 22.04 LTS act as a packet generator and packet sink.

B. Experimental Setup

We aim to measure the packet transmission delay in the described 5G-TSN network for DL direction. The delay measurement points within the considered system, i.e., D_{emp} as defined in Eq. (4), are illustrated in Fig. 4. Specifically, these points are the output ports of the TSN switches MS and SL and are marked with a red dot. Network traffic is generated

at the Tx server with *packETH* tool. Packets are tagged with PCP 2 for DC and with PCP 0 for BE to be then matched to the uRLLC and eMBB 5G slices, respectively. The DC packet size is fixed to 200 Bytes and the generation rate is set to the maximum rate to allow the availability of packets at the TSN MS queue at all times, with no impact on their discarding. In contrast, BE packets are Maximum Transmission Unit (MTU)-sized, i.e., 1500 Bytes, and generated at a constant speed of 30 Mbps. Nevertheless, due to WR-Z16's queue size limitations explained above, a maximum throughput of 1.6 Mbps for *delay-critical* traffic has been fixed by window sizing for TAS experiments to ensure no packet is discarded/lost when it finds a queue crowded. For each experiment, traffic was captured for 15 minutes, ensuring a minimum of 250,000 samples.

To measure packet transmission delay, we employed the WR-Z16 timestamp probes. These probes dump the sequence number allocated within the first 4 Bytes of the UDP payload of a packet and the timestamp when it left the port to a CSV file. With the file probed both at the TSN MS and the TSN SL, the latencies for every packet can be calculated as the difference between them, identified by their sequence number. Note that, for accurate delay calculation, both TSN switches must be correctly synchronized, so PTP packets also join the uRLLC slice.

VI. PERFORMANCE RESULTS

In this work, we have carried out three different experiments. Firstly, we have measured the 5G jitter between TSN switches to check the effect of increments on the load. Secondly, the offset between GCL schedules performed at TSN switches has been swept according to the worst-case latency value. Finally, for this last offset configuration, the periodicity has been also swept keeping the same throughput.

A. Jitter Analysis Based on Throughput

Fig. 5 presents the resulting CDF of latency between TSN switches MS and SL for increasing throughput via its window size, $w_{DC}^{MS,SL}$ (defined in Eq. (2)), in a TSN-enabled network incorporating a 5G bridge. The TAS is configured at TSN MS only to measure the D_{emp} delay (Fig. 2). The *network cycle* is fixed at 30 ms. A sweep in throughput steps of 300 kbps, from 350 kbps to 1.55 Mbps, results in window sizes $w_{DC}^{MS,SL}$ of 10.5 μ s to 46.5 μ s, respectively. It has been proven that configurations with smaller window sizes exhibit the lowest latencies, whereas larger windows introduce a slight rightward delay shift as $w_{DC}^{MS,SL}$ increases. This behavior suggests that increasing this window substantially affects scheduling efficiency, potentially due to buffering mechanisms within the 5G bridge. This effect takes place for each DC packet while packets ahead in the queue are still awaiting their transmission, as shown with Eq. (4). The convergence of all distributions suggests averages between 6.5 ms and 7.25 ms but a much higher maximum value at 17 ms. However, we conclude with a well-defined latency upper bound near 15 ms for that 99.9% reliability as commented in Section IV. This value provides the empirical offset δ to be applied between MS and SL.

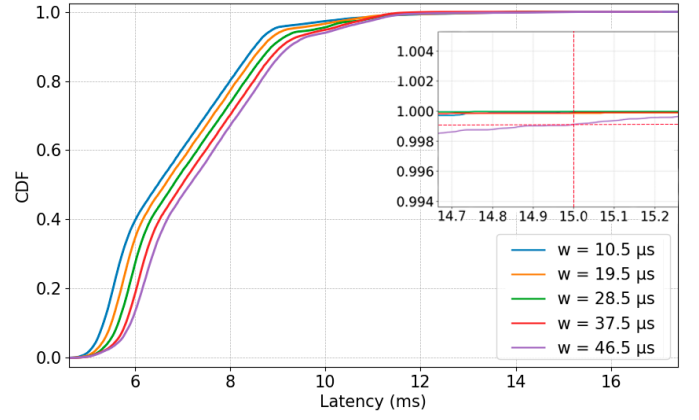


Fig. 5. 5G latencies CDF for different windowed loads

B. Jitter Analysis Based on Offset Between TSN MS and SL

This second experiment has focused on the highest latency configuration to characterize the value of the offset δ that best fits to optimize latency for DC traffic. The time duration of the window $w_{DC}^{MS,SL}$ and the period of the TSN MS switch are kept constant. Thus, the size of $w_{DC}^{MS,SL}$ is 46.5 μ s, and the *network cycle* T_C is 30 ms for both TSN MS and SL. Then, the configuration of the TSN slave switch is identical, except that we sweep the offset δ over the range [5, 30] ms. The step is 5 ms. Fig. 6 shows the Complementary Cumulative Distribution Function (CCDF) of the results, where latencies decrease as its offset gets closer to the worst-case latency measured in the previous experiment, i.e., 15 ms. However, at this point, latencies start to jump the equivalent of T_C , i.e., 30 ms, as packets now have to wait until the next window for DC traffic in the following *network cycle*. This means that ICI cumulative effect is occurring in the queue, the same as seen in Section IV. Note that the effect of packet accumulation for $\delta = 15$ ms arises at this point as this jump probability is around 0.7%, higher than the 0.1% objective set in the previous experiment. The lower the offset, the higher the probability of this jump. For $\delta = 5$ ms, the probability of this latency jump is over 90% as this is too tight. A lower value of offset increases this

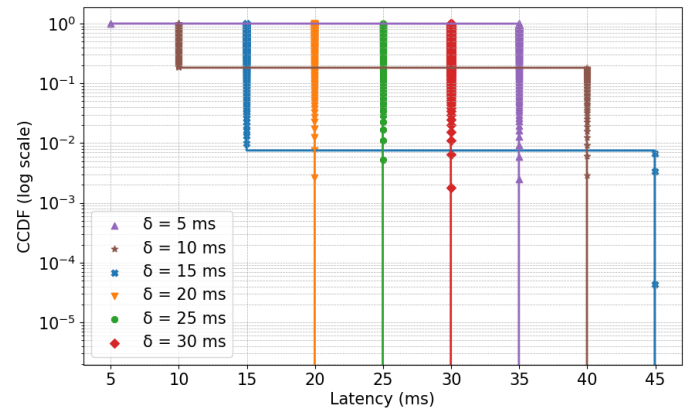


Fig. 6. Offset sweep for fixed period and window values

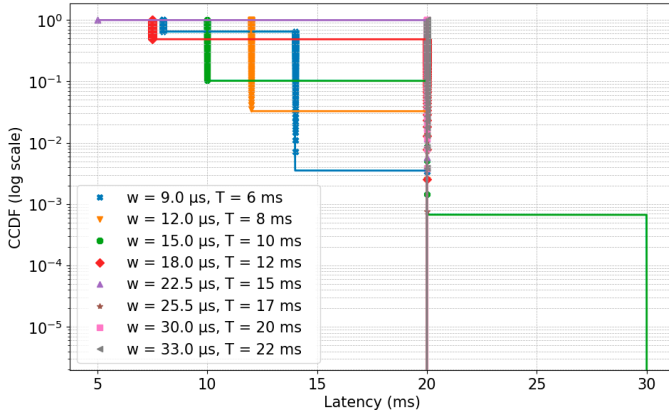


Fig. 7. Window and period sweep for fixed offset

probability until almost every packet arrives to TSN slave later than expected. On the other hand, the offset value of $\delta = 20$ ms optimizes the latency without a deeper sweep.

C. Jitter Analysis Based on Network Cycle

In this third and last experiment, we used the same setup as in the previous experiment, i.e., $\delta = 20$ ms, but we now sweep the *network cycle* T_C instead of the offset δ . To maintain the throughput, we calculate a proportional window $w_{DC}^{SL,Rx}$ at the TSN SL for each T_C value. As a contingency measure, we applied an additional 25% to $w_{DC}^{SL,Rx}$ displayed in Fig. 7 at the TSN SL to avoid overloading the queue at the expense of slightly reducing bandwidth for the BE traffic. Decreasing T_C , and therefore increasing the frequency of *transmission window* $w_{DC}^{SL,Rx}$, results in lower latencies than the fixed offset δ , aligned with the corresponding CDF. However, this may limit the total bandwidth for BE traffic as the number of windows and the *guard bands* increase per unit of time. Additionally, this may cause the ICI effect (Section IV), and packets will start to accumulate between network cycles until the queue is saturated. In our results, T_C values below 15 ms start suffering ICI, in which lower latencies can be seen like the case of 7.25 ms for $T_C = 12$ ms. However, these probabilities are very low, and the corresponding latencies increase rapidly. For $T_C = 6$ ms and $T_C = 10$ ms, the latency increases to a third window at 20 ms and 30 ms, respectively; which implies some packets are retained in queue for two network cycles. In the case of $T_C = 8$ ms this effect does not occur. The lowest latency value for each T_C depends on its alignment with the offset δ . Thus, for the same traffic load, TAS modifies the traffic pattern in 5G and, therefore, the latencies of the 5G-TSN network.

VII. CONCLUSIONS AND FUTURE WORK

In this work, we presented an empirical analysis of the impact of 5G jitter on the performance of IEEE 802.1Qbv in an integrated 5G-TSN network. Firstly, we have provided background on aspects of industrial 5G-TSN networks, especially those related to elements that compose this kind of network and its applications. Secondly, we have analyzed, formulated, and modeled the effect of 5G jitter on the TAS mechanisms

through the associated constraints. We have focused this on the DL communication between two TSN switches interconnected through a 5G bridge and transferred to our testbed equipment, including a set of TSN translators. Finally, we have identified and tested the key configuration parameters required to optimize the TAS scheduling for this integration in a 5G-TSN environment. Our experiments show that the offset between TSN switches plays a key role in achieving determinism, beyond the latencies measured in the 5G system.

Our line of future work is intended to perform additional experiments related to the periodicity and the ICI effects to optimize traffic scheduling for general applications.

REFERENCES

- [1] W. Saad, M. Bennis, and M. Chen, "A Vision of 6G Wireless Systems: Applications, Trends, Technologies, and Open Research Problems," *IEEE Netw.*, vol. 34, no. 3, pp. 134–142, 2020.
- [2] "Time Sensitive Networks for Flexible Manufacturing Testbed Characterization and Mapping of Converged Traffic Types." White Paper, 2019.
- [3] 5G-ACIA, "Integration of 5G with Time-Sensitive Networking for Industrial Communications." White Paper, Feb. 2021.
- [4] Z. Satka, M. Ashjaei, H. Fotouhi, M. Daneshmand, M. Sjödin, and S. Mubeen, "A comprehensive systematic review of integration of time sensitive networking and 5G communication," *J. Syst. Archit.*, vol. 138, p. 102852, 2023.
- [5] J. Sasiain, D. Franco, A. Atutxa, J. Astorga, and E. Jacob, "Towards the Integration and Convergence Between 5G and TSN Technologies and Architectures for Industrial Communications: A Survey," *IEEE Commun. Surv. Tutor.*, pp. 1–1, 2024.
- [6] P. M. Rost and T. Kolding, "Performance of Integrated 3GPP 5G and IEEE TSN Networks," *IEEE Commun. Stand. Mag.*, vol. 6, no. 2, pp. 51–56, 2022.
- [7] A. Larrañaga, M. C. Lucas-Esteban, I. Martínez, I. Val, and J. Gozalvez, "Analysis of 5G-TSN Integration to Support Industry 4.0," in *IEEE ETFA*, vol. 1, pp. 1111–1114, 2020.
- [8] S. Rodrigues and J. Lv, "Synchronization in Time-Sensitive Networking: An Introduction to IEEE Std 802.1AS," *IEEE Commun. Stand. Mag.*, vol. 6, no. 4, pp. 14–20, 2022.
- [9] R. Debnath, M. S. Akinci, D. Ajith, and S. Steinhorst, "5GTQ: QoS-Aware 5G-TSN Simulation Framework," in *IEEE VTC-Fall*, pp. 1–7, 2023.
- [10] J. Fontalvo-Hernández, A. Zirkler, and T. Bauschert, "Determinism in Industrial Converged Networks: Evaluating Approaches to Jitter Mitigation in 5G and TSN Integration," in *IFIP Networking*, pp. 744–749, 2024.
- [11] D. Wang, X. Jin, Z. Feng, and Q. Deng, "B-UFS: Uniform Resource Metric-Based Periodic Flow Scheduling in 5G-TSN Integrated Network," in *IEEE SIES*, pp. 140–147, 2024.
- [12] A. Aijaz and S. Gufran, "Time-Sensitive Networking over 5G: Experimental Evaluation of a Hybrid 5G and TSN System with IEEE 802.1Qbv Traffic," in *NoF*, pp. 101–105, 2024.
- [13] 3GPP TS 23.501, "System architecture for the 5G System (5GS) (Release 19)," June 2024.
- [14] "IEEE Standard for a Precision Clock Synchronization Protocol for Networked Measurement and Control Systems," *IEEE Std 1588-2019*, pp. 1–499.
- [15] 3GPP Technical specification (TS) TS22.104, "Service requirements for cyber-physical control applications in vertical domains (V17.7.0 Release 17)," 2022.
- [16] Y. Oge *et al.*, "Software-Based Time-Aware Shaper for Time-Sensitive Networks," *IEICE Trans. Commun.*, vol. 103, no. 3, pp. 167–180, 2020.
- [17] R. Serna Oliver, S. S. Craciunas, and W. Steiner, "IEEE 802.1Qbv Gate Control List Synthesis Using Array Theory Encoding," in *IEEE RTAS*, pp. 13–24, 2018.
- [18] J. Walrand, "A Concise Tutorial on Traffic Shaping and Scheduling in Time-Sensitive Networks," *IEEE Commun. Surv. Tutor.*, vol. 25, no. 3, pp. 1941–1953, 2023.
- [19] J. Lin *et al.*, "Rethinking the Use of Network Cycle in Time-Sensitive Networking (TSN) Flow Scheduling," in *2022 IEEE/ACM 30th Int. Symp. Quality of Service (IWQoS)*, pp. 1–11, IEEE, 2022.